REVISTA MATÉRIA V.27 N.04
ISSN 1517-7076 articles e20220172, 2022

Numerical analysis of combined optimization of turbine runner flow pattern and shafting System

Xuejun Zhou[1], Jiuming Xie[1], Meiping Zhang[2]

[1]Tianjin Sino-German University of Applied Science. Tianjin, 300350 China.
[2]Tianjin University of Technology. Binshui Xidao, Xiqing District, Tianjin, China.
e-mail: zhouxuejun1978@163.com, xiejiuming1983@163.com, zhangmeiping0712@163.com

ABSTRACT

This paper attempts to solve the turbine failures reported by a hydropower station, namely, the violent vibration in the runner region under a special working condition and the blade cracking on the outlet edge near the lower ring. For this purpose, the entire flow channel of the turbine was simulated by computational fluid dynamics (CFD) on ANSYS, and the runner strength and mode of shaft assembly system (SAS) were computed by the liquid-solid coupling algorithm. The calculation results show that severe low (negative) pressure appeared on the outlet edge near the lower ring, excess stress was observed in that area, and the resonance occurred as the fifth and sixth order natural frequencies of the SAS were the same with the rotation frequencies of the blade. On this basis, the original blade was modified repeatedly. Through the modification, the flow field distribution in the runner region and the blade strength were both greatly improved, and the SAS natural frequencies were kept away from the various external excitation frequencies, laying a solid basis for the safe and stable operation of the turbine.

Keywords: Francis turbine; Shaft assembly system (SAS); Computational fluid dynamics (CFD); Liquid-solid coupling algorithm; Vibration mode.

1. INTRODUCTION

The Francis turbine may vibrate during operation, due to the interaction between component surface and the fluid [1]. The turbine structure will resonate with the external excitation, when its natural frequency is the same or multiples of the frequency of the latter. Sustained vibration will cause fatigue damage to the components of the turbine, as shown in Figure 1. Early structural damage occurs to the components with irrational design. After all, an irrational structure means an unreasonable distribution of the flow field, and the resulting pressure difference will lead to stress concentration in local areas.

Most studies on turbine vibration only focus on the runner [2–5]. In actual Francis turbines, however, most vibrations and damages occur in the shaft assembly system (SAS). This calls for in-depth research into the SAS. The runner is a flow passage component within the SAS. Thus, the wet mode of the runner must be included in the mode calculation of the SAS. Traditionally, the features of wet mode can be computed in two ways. Firstly, the natural frequency in water can be obtained by multiplying the natural frequency in air with an empirical influence coefficient. Nonetheless, the calculation result may deviate greatly from the real-world situation, because the natural frequency of the runner in the flow channel is affected by multiple factors [6, 7]. Secondly, the effect of the fluid on the runner can be approximated by the additional mass the assembly brings to the total mass matrix. This method also has certain limitations, as it fails to change the system stiffness [8, 9].

This paper mainly deals with the following turbine failures reported by a hydropower station: (1) the runner region vibrated violently when the turbine generated 10% extra power under the maximum head; (2) The blade root cracked as shown in Figure 1. In the light of the failures, two calculation models were established, one for the water in the entire flow channel, and the other for the SAS. Firstly, the water model was subjected to numerical simulation by computational fluid dynamics (CFD), revealing the law of flow field distribution around the cracked blade. Taking the CFD simulation results as the boundary conditions, the runner strength and mode of the SAS were computed by the fluid-solid coupling algorithm. Based on the computed results, the

Corresponding Author: Jiuming Xie Received on 13/07/2022 Accepted on 21/09/2022

DOI: https://doi.org/10.1590/1517-7076-RMAT-2022-0172

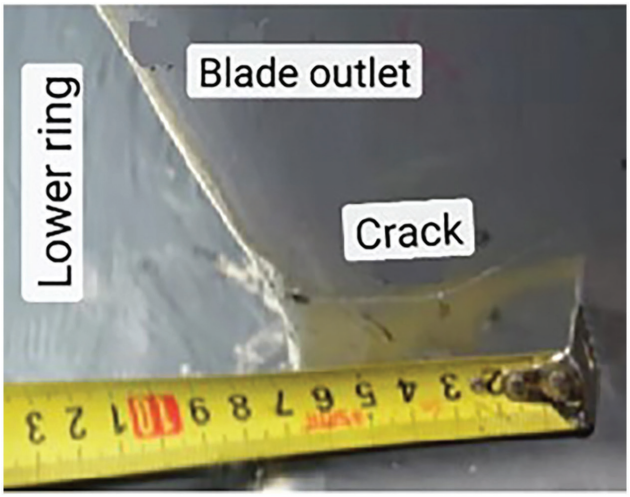

Figure 1: Blade cracking.

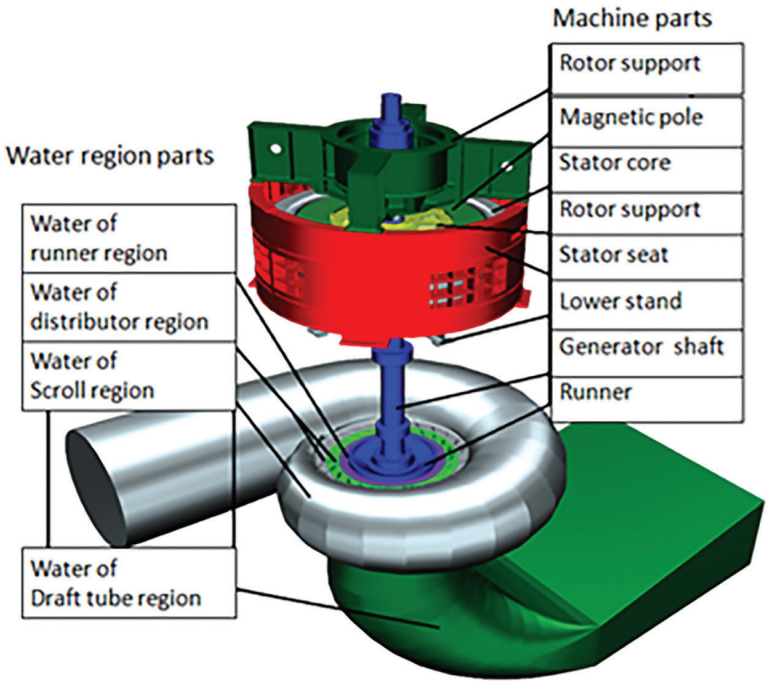

Figure 2: The water model and the SAS model.

blade was modified several times and verified through calculation, without sacrificing the turbine performance. The final blade design clearly improved the flow distribution around the blade, and greatly enhanced the runner strength, producing a new SAS that does not resonate at various excitation frequencies. In this way, the reported failures were successfully resolved.

2. CALCULATION MODELS

Two calculation models were established, one for the water in the entire flow channel, and the other for the SAS. The water model covers the water in the volute casing, that in the guide vanes, that in the runner region and that in the tail race. The SAS model includes both rotating parts (e.g. rotor support, magnetic pole, magnetic yoke, motor shaft, turbine shaft, and runner) and static parts (e.g. upper bracket, stator frame, stator core, and lower bracket), making the boundaries for SAS finite-element calculation more realistic. The two models are illustrated in Figure 2.

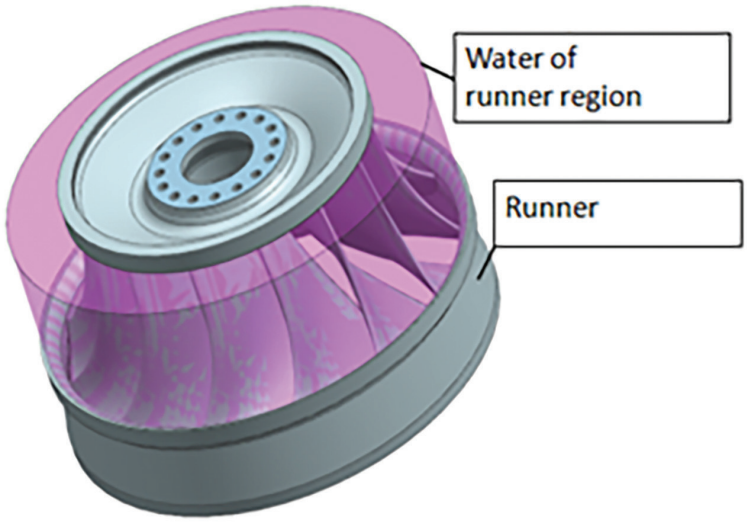

Figure 3: The liquid-solid coupling model for the runner region.

In the calculation models, the water in the runner region and the runner of the SAS were combined into the liquid-solid coupling model in Figure 3.

3. ESTALISHMENT AND SOLUTION OF SYSTEM GOVERNING EQUATIONS

3.1. Governing equations for liquid-solid coupling system

The Navier-Strokes equations can be converted into the following nondimensional form [10]:

$$\frac{\partial u_i}{\partial x_i} = 0 \tag{1}$$

$$\frac{\partial u_i}{\partial t} + u_i \frac{\partial u_i}{\partial x_j} = b_i - \frac{\partial p}{\partial x_i} + \frac{1}{R_e} \nabla^2 u_i \tag{2}$$

where u_i are the components u, v and w of the fluid velocity vector in the x, y and z directions; p is the pressure; R_e is the Reynolds number.

From formulas (1) and (2), the global matrices for pressure and velocity can be respectively derived as:

$$AU + BUU + CP + DU = E + F \tag{3}$$

$$GU = H \tag{4}$$

where $U = [uv\omega]T$; A, B, C, D, E and F are the global matrices of the mass, convection, pressure, loss, body force and surface force, respectively; G and H are the global matrices of the continuous velocity and the boundary velocity, respectively.

Considering the elasticity of flow passage components, the finite-element equation for the overall structural vibration of elastomer was constructed as [11]:

$$M\delta + C\delta + K = P \tag{5}$$

The CFD simulation of the water shows that, the water pressure field changes the vibration mode of flow passage components, which in return affect the flow field distribution in the water. On the liquid-solid coupling surface, the water and the SAS have the same velocity and pressure. Therefore, the solution of the liquid-solid coupling model is equivalent to that of formulas (3)~(5).

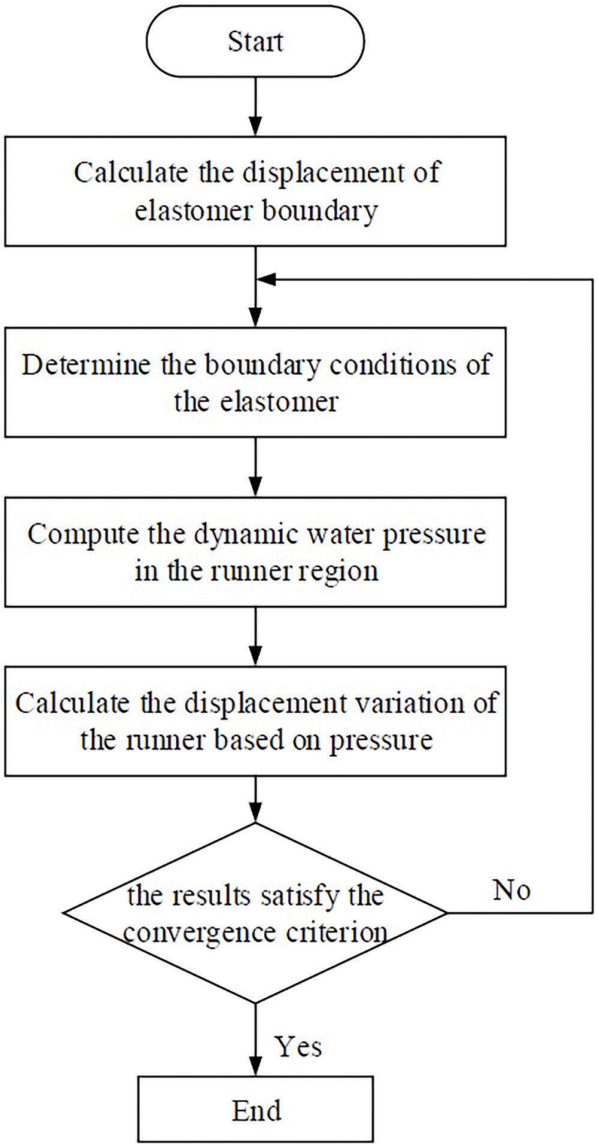

Figure 4: The flow chart of solve for liquid-solid coupling model.

3.2. Solving the liquid-solid coupling model

In the steady condition, the water flows in the runner region, and was thus considered as compressible ideal fluid. Then, the liquid-solid coupling model can be solved by the following flow chart in Figure 4.

In Figure 4, the boundary condition of the elastomer by:

$$\frac{\partial F}{\partial x}u+\frac{\partial F}{\partial y}v+\frac{\partial F}{\partial z}w+\frac{\partial F}{\partial t}=0 \tag{6}$$

4. CALCULATION RESULTS OF THE ORIGINAL TURBINE

4.1. Blade pressure

The entire flow channel of the original turbine was numerically simulated to obtain the cloud chart on blade pressure field (Figure 5).

4.2. Blade strength

The SAS model was subjected to finite-element calculation on ANSYS by the liquid-solid coupling algorithm. The resulting blade strength in the runner region is presented in Figure 6 below.

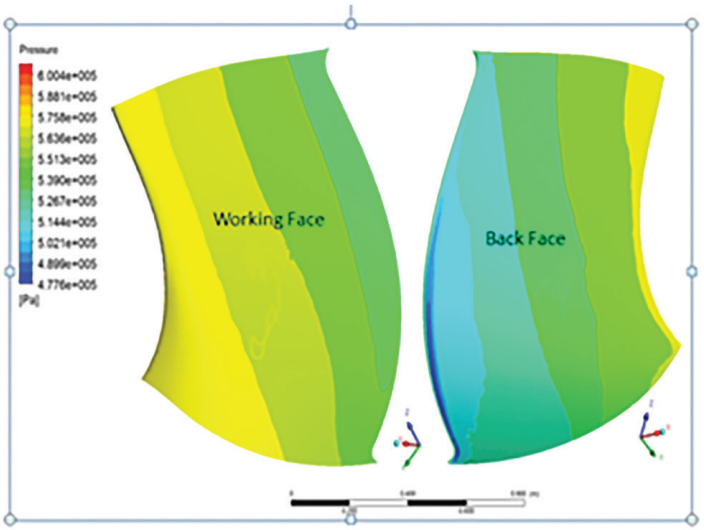

Figure 5: Cloud chart on blade pressure.

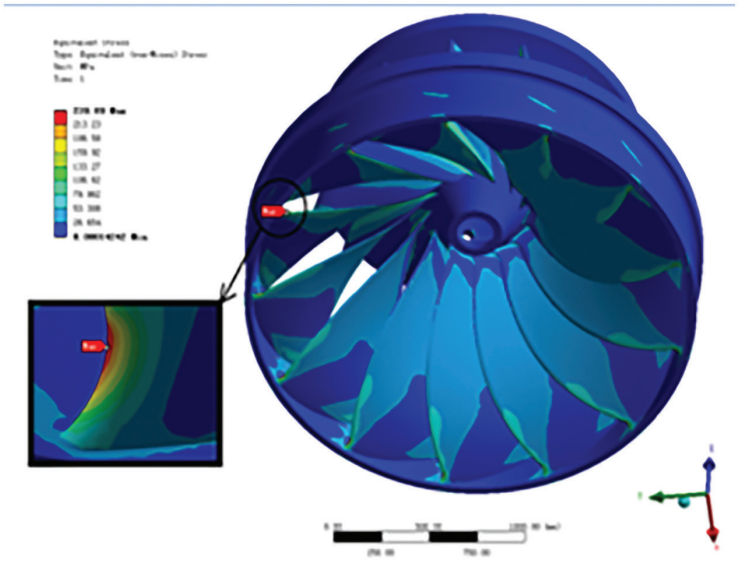

Figure 6: Blade strength.

Table 1: The natural frequencies in the first six orders of the SAS.

ORDER NUMBER	NATURAL FREQUENCY(*f*/*HZ*)
1	15.592
2	17.759
3	43.453
4	46.431
5	64.652
6	66.348

4.3. SAS vibration modes

Using liquid-solid coupling algorithm, the natural frequencies in the first six orders of the SAS and the corresponding vibration modes were computed, under the assumption that the turbine generates 10% extra power under the maximum head. The calculated results are listed in Table 1, and the obtained vibration modes are displayed in Table 1 and Figure 7.

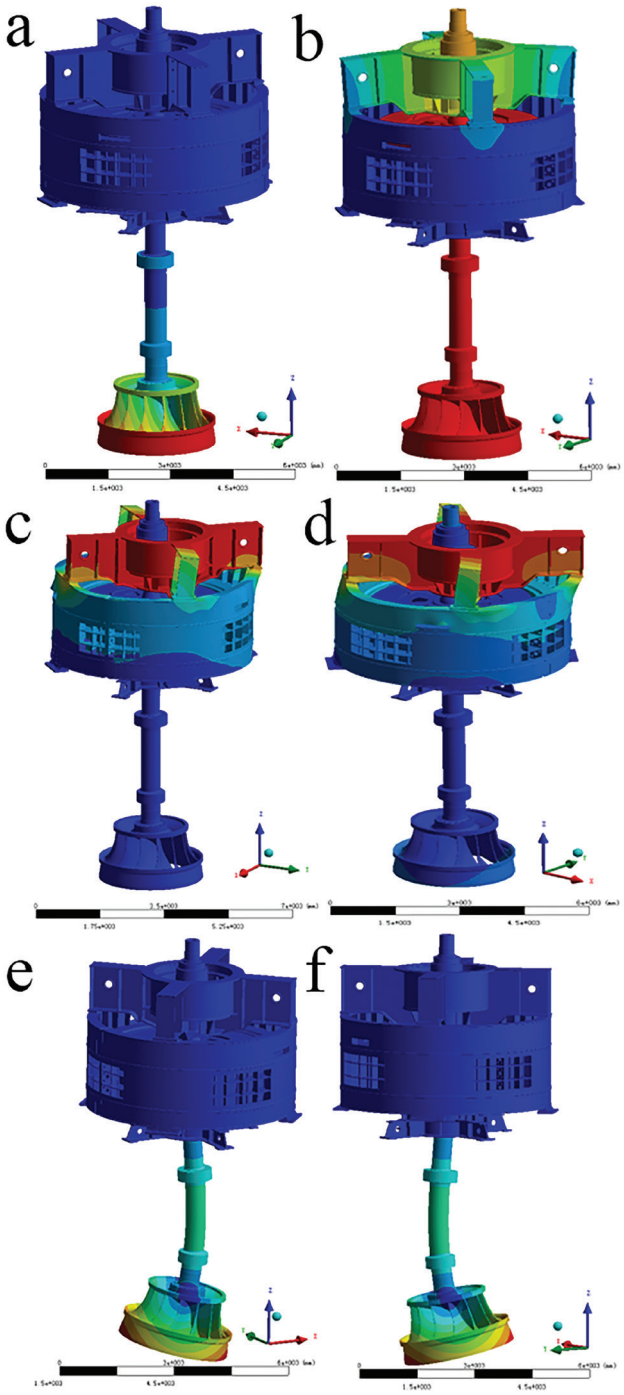

Figure 7: The vibration modes in the first six orders of the SAS.

4.4. Results analysis

(1)The static pressure distribution of the blade shows that the pressure surface of the blade had a greater pressure than the suction surface. On the suction surface, the pressure was extremely low (even negative) on the outlet edge of the blade near the lower ring. The pressure was much lower than the immediate surroundings, resulting in a huge pressure difference between the two sides of the blade. This low-pressure area is exactly the cracked zone of the blade.

(2)According to finite-element calculation, the maximum stress in the runner region stood as 204.8MPa, exceeding the safe level required for normal working condition in relevant Chinese national standards [12]. In addition, the maximum stress appeared at the cracked zone of the blade, which agrees with the flow field calculation results.

Table 2: The external excitation frequencies of the original turbine.

EXCITATION FEQUENCY	CALCULATION RESULTS(*HZ*)
Frequency conversion	$f = \frac{n}{60} = 5$
E.F. of Vortex Belt in Tailwater	$f_{B.T} = \frac{0.20\ 0.50\ n}{60} = 1.0 \sim 2.5$
E.F. of guide vane Rotation	$f_{G.R.} = Z_0 \frac{n}{60} = 120$
E.F. of Carmen Vortex [13]	$f_{c.v.} = sh\frac{W}{\delta} = 83132$ *sh*-0.18~0.25;
E.F. of Thrust Bearing	$f_{T.B.} = \frac{nP}{60} = 40$
E.F. of Blade Rotation	$f_{B.R} = \frac{nZ_1}{60} = 65$

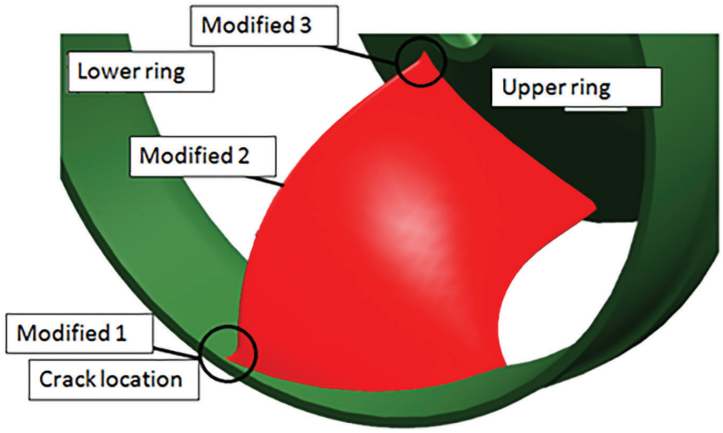

Figure 8: The main modification parts.

(3)Through the calculation of natural frequencies of the SAS, it is clear that the SAS vibrated along the axial direction in the first and second modes; the rotor support vibrated along the vertical direction in the third and fourth modes; the runner vibrated along the vertical direction in the fifth and sixth modes.

The external excitation frequencies were calculated based on the known parameters of the turbine: the rotation speed n of 300r/min, the number of blades Z_1 of 13, the number of bushes P of 8, and the number of guide vanes Z_0 of 24. The calculated results are listed in Table 2 below.

Comparing the natural frequencies and external excitation frequencies of the original turbine, it is obvious that the fifth and sixth order natural frequencies of the SAS are close to the blade rotation frequency. The fifth and sixth vibration modes are mainly demonstrated by the vibration of the runner along the vertical direction, and the maximum amplitude appears at the junction between the outlet edge and the lower ring, which is the cracked zone of the blade. This is the root cause of the blade cracking and the vibration in the runner region.

5. MODIFICATION PLAN

The blades of the original turbine were modified according to the above calculation results. The modification principle is to change the structure and weight of the SAS by reshaping the original blade. In this way, the natural frequencies of the SAS will be changed, and kept away from various external excitation frequencies, that is, eliminating resonance. The main modification parts of the original blade are illustrated in Figure 8.

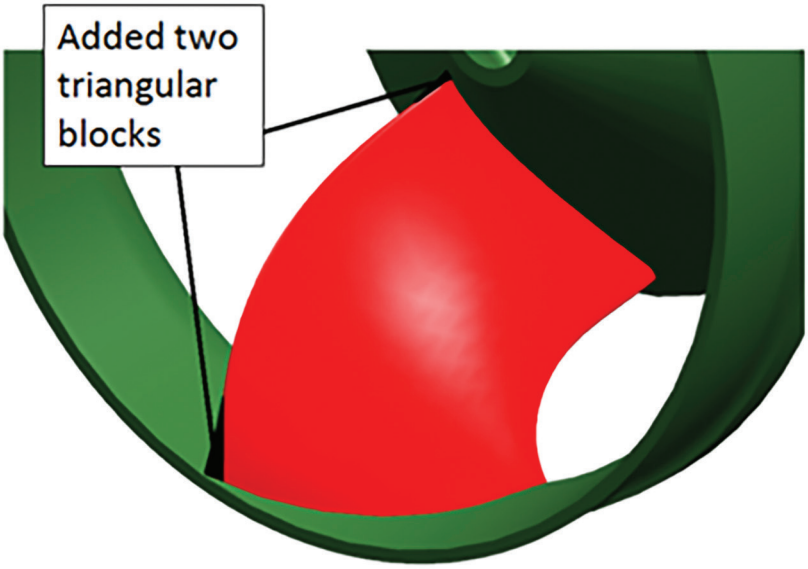

Figure 9: Step 1 of modification.

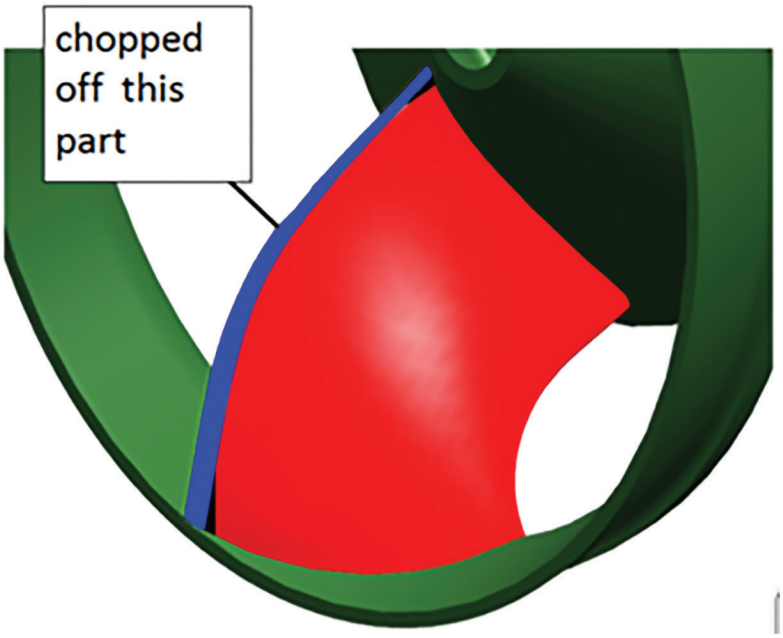

Figure 10: Step 2 of modification.

The modification is carried out in two steps:

Step 1: The finite-element results on the runner show excessive stresses near the upper rim and the lower ring, indicating that the two parts should be enhanced. Thus, triangular blocks were welded to the two parts [14] (Figure 9).

Step 2: The pressure field distribution of the blade shows that the pressure was extremely low on the outlet edge of the blade near the lower ring. Hence, this part was chopped off and then the outlet edge was polished smooth (Figure 10).

Figure 11: The new blade.

The new blade was obtained through repeated modifications, flow field calculation and finite-element computation (Figure 11).

6. CALCULATION RESULTS OF THE MODIFIED TURBINE

6.1. Blade pressure

The entire flow channel of the modified turbine was numerically simulated to obtain the cloud chart on blade pressure field (Figure 12).

6.2. Blade strength

The blade strength of the modified turbine was subjected to finite-element calculation. The results are shown in Figure 13.

6.3. SAS vibration modes

The natural frequencies in the first six orders of the SAS in the modified turbine and the corresponding vibration modes were computed, under the assumption that the turbine generates 10% extra power under the maximum head. The calculated results are listed in Table 3, and the obtained vibration modes are displayed in Figure 14.

6.4. Results analysis

(1)The static pressure distribution (Figure 11) shows that the pressure surface of the blade generally had a greater pressure than the suction surface. As shown in Figure 11b, the modified blade enjoyed a rational distribution of flow field on the outlet edge near the lower ring, eliminating the severe low (negative) pressure before the modification.

(2)According to finite-element calculation, the maximum stress in the runner region of the modified turbine stood as 130.04MPa, which falls within the safe level required for normal working condition in relevant Chinese national standards [12].

(3)Through the calculation of natural frequencies of the SAS, it is learned that the new turbine had basically the same SAS vibration modes with the original turbine, but differed greatly from the original turbine in the nature frequencies of the SAS. The comparison between Tables 1 and 3 shows that the first to sixth order natural frequencies of the SAS in the modified turbine deviated from the external excitation frequencies. In the fifth and sixth orders, the vibration frequencies of the runner in the modified turbine were different from the blade rotation frequencies, despite the lack of vibration isolation. Thus, the modified blade will not crack like the original one.

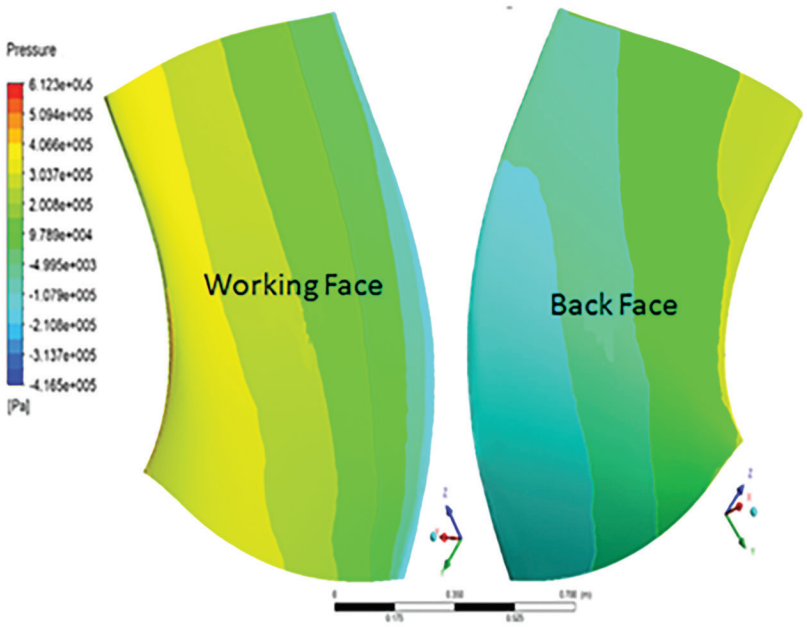

Figure 12: Cloud chart on blade pressure.

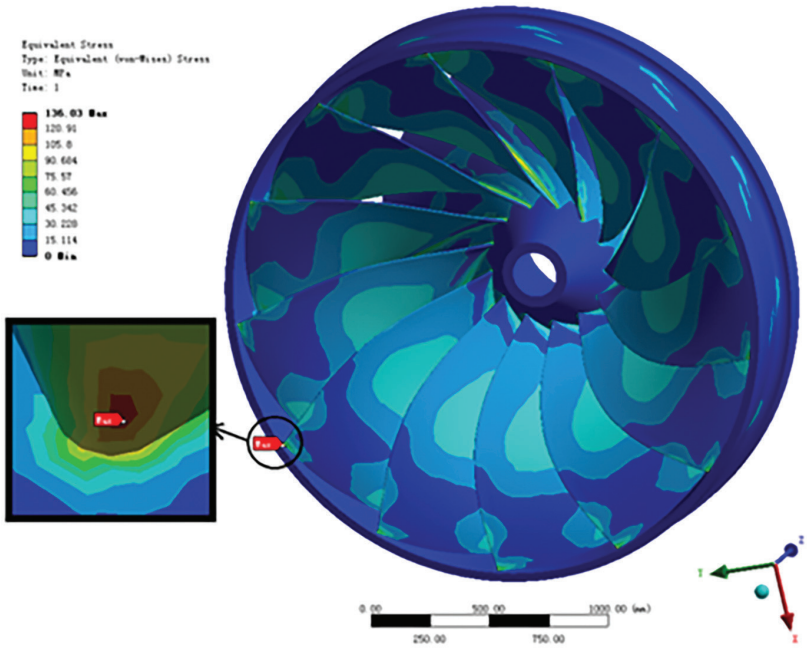

Figure 13: Blade strength.

Table 3: The natural frequencies in the first six orders of the SAS.

ORDER NUMBER	NATURAL FREQUENCY(*f*/*HZ*)
1	18.764
2	19.547
3	49.132
4	51.436
5	72.765
6	74.264

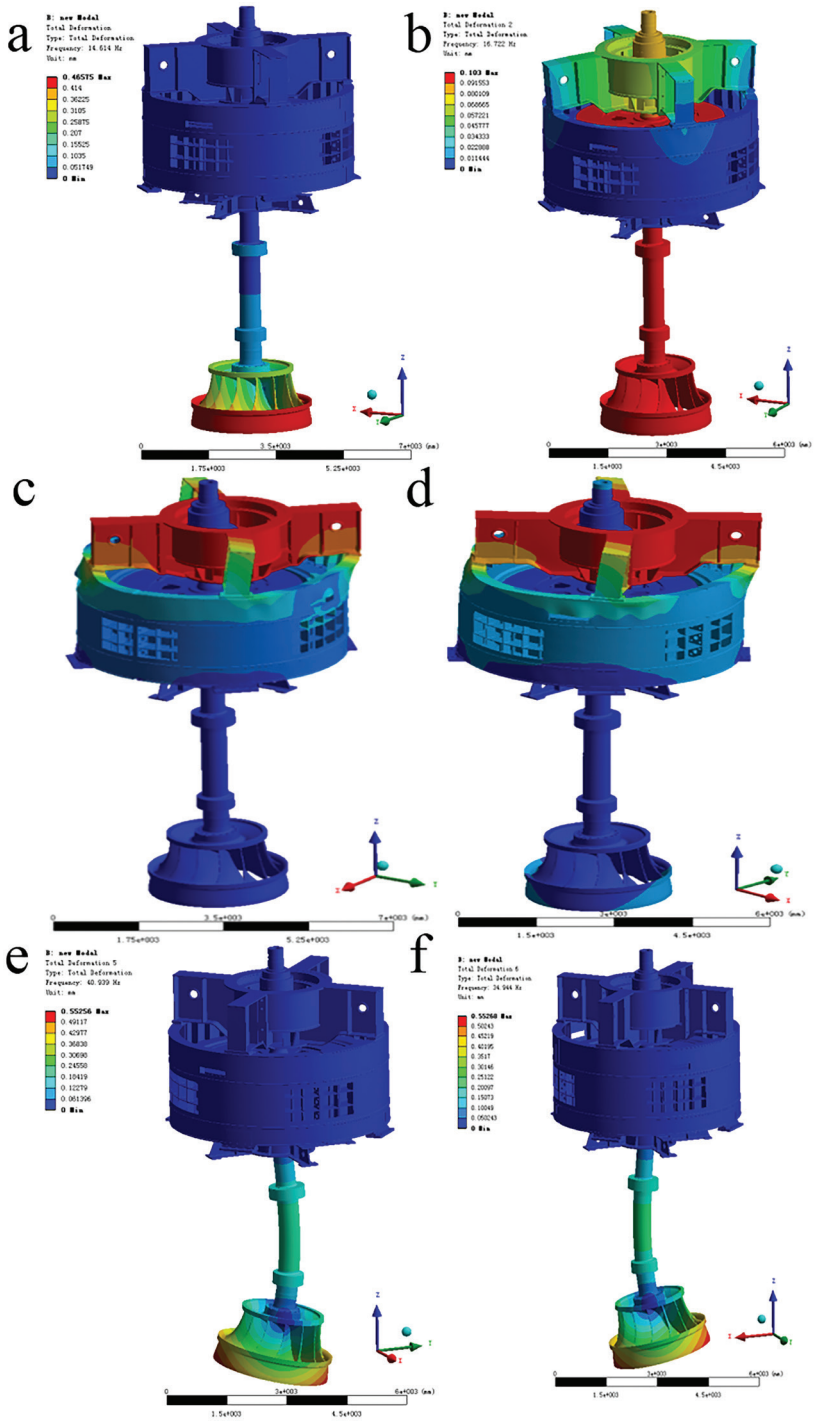

Figure 14: The vibration modes in the first six orders of the SAS.

7. CONCLUSIONS

In the light of the turbine failures reported by a hydropower station, this paper calculates and analyzes the flow field in the entire flow channel, the runner strength and the SAS vibration features based on ANSYS. The blade of the original SAS was modified according to the calculation results. The modified SAS managed to avoid the turbine failure. The following conclusions were drawn from the research:

(1)Most studies on turbine vibration only focus on the runner. In actual Francis turbines, however, most vibrations and damages occur in the SAS, the component responsible for rotation and energy conversion. Therefore, the SAS must be fully investigated to solve the vibration of the turbine.

(2)The runner is a flow passage component within the SAS. The natural frequencies of the runner in water changes with vibration modes. As a result, the liquid-solid coupling algorithm was adopted to determine the natural frequencies of the runner region in the SAS. This algorithm overcomes the limitation and error of traditional algorithms.

(3)Based on the flow field and finite-element results, the weak parts of the blade and the area with irrational flow field distribution were modified, changing the structure and weight of the SAS. In this way, the natural frequencies of the SAS will be changed, and kept away from various external excitation frequencies, that is, eliminating resonance.

(4)Based on the computed results, the blade was modified several times and verified through calculation, without sacrificing the turbine performance. The final blade design clearly improved the flow distribution around the blade, and greatly enhanced the runner strength, producing a new SAS that does not resonate at various excitation frequencies. The reported failures were successfully resolved.It lays a solid foundation for the safe and stable operation of steam turbine.

8. BIBLIOGRAPHY

[1] ZHANG, L., ZHANG, H., "Analysis of transverse vibrating characteristics of francis hydro turbine blades in steady flow.", *Water Resources and Power*, v. 22, n. 3, pp. 78–81, 2004.

[2] YUN, L., WU, C., XIE, Y., "Fluid-aerodynamics performance investigation of dynamic air cushion wing-in-ground effect craft", *Engineering and Science*, v. 2, n. 4, pp. 48–52, 2000.

[3] YANG, H., "The development of wing-in-surface effect crafts and a outlook about their application", *Flight Mechanics*, v. 19, n. 1, pp. 13–17, 2001.

[4] QU, Q., LIU, P., "Numerical simulation and analysis of aerodynamics of WIG craft in cruise over ground", *Acta Aeronauticaet et Astronautica Sinica*, v. 27, n. 1, pp. 16–22, 2006.

[5] HONG, L., XU, B., HONG, F., *et al*., "Simulation of 3 -D flow around WIG with nonlinear k -ɛturblence model", *Journal of Ship Mechanics*, v. 7, n. 1, pp. 23–32, 2003.

[6] XIAO, R., WEI, C., HAN, F., *et al*., "Study on dynamic analysis of the Francis Turbine Runner", *Large Motor Technology*, n. 7, pp. 41–43, 2001.

[7] GU, C., YAO, X., CHEN, Q., "Study on fluid-solid danymic characteristics for the component of hydraulic turbines", *Large Motor Technology*, n. 6, pp. 47–52, 2001.

[8] LIU, Z., SUN, Y., XIE, S., "Structural dynamic character and its response analysis in fluid medium", *Journal of Shanghai Jiaotong University*, v. 29, n. 4, pp. 7–16, 1995.

[9] TAO, F., YANG, Y., LIU, Z., "Research on natural frequencies and dynamical response of submerged moving structure", *Journal of Shanghai Jiaotong University*, v. 31, n. 7, pp. 137–143, 1997.

[10] WANG, C., "Dimensionalization of Navier-Stokes equations", *High-tech Enterprises in China*, v. 3, n. 3, pp. 61–62, 2016.

[11] MOAVENI, S., *Finite element analysis-ANSYS theory and application*, Beijing, Electronic Industry Press, 2008.

[12] GENERAL ADMINISTRATION OF QUALITY SUPERVISION, INSPECTION AND QUARANTINE OF THE PEOPLE'S REPUBLIC OF CHINA, China National Standardization Management Committee, *Basic technical conditions of hydraulic turbines (GB15468-2006)*, Beijing, 2006.

[13] QIU, H., *Research on key technologies of condition-based maintenance of hydraulic machinery*, Beijing, Tsinghua University, 2002.

[14] ZHAO, Y., "Verification and analysis of the process of turbine runner replacing triangular block in jinghong hydropower station", *Mechanical Engineering*, n. 2, pp. 143–144, 2013.